Aerosol Science and Technology, 45:510–521, 2011

ISSN: 0278-6826 print / 1521-7388 online
DOI: 10.1080/02786826.2010.547538

BNL-94767-2011-JA

Electrical Mobility Spectrometer Using a Diethylene Glycol Condensation Particle Counter for Measurement of Aerosol Size Distributions Down to 1 nm

Jingkun Jiang,[1,4] Modi Chen,[1] Chongai Kuang,[1,2] Michel Attoui,[3] and Peter H. McMurry[1]

[1]*Department of Mechanical Engineering, University of Minnesota, Minneapolis, Minnesota, USA*
[2]*Atmospheric Science Division, Brookhaven National Laboratory, Upton, New York, USA*
[3]*University of Paris XII, Paris, France*
[4]*Department of Environmental Science & Engineering, Tsinghua University, Beijing, China*

We report a new scanning mobility particle spectrometer (SMPS) for measuring number size distributions of particles down to ∼1 nm mobility diameter. This SMPS includes an aerosol charger, a TSI 3085 nano differential mobility analyzer (nanoDMA), an ultrafine condensation particle counter (UCPC) using diethylene glycol (DEG) as the working fluid, and a conventional butanol CPC (the "booster") to detect the small droplets leaving the DEG UCPC. The response of the DEG UCPC to negatively charged sodium chloride particles with mobility diameters ranging from 1–6 nm was measured. The sensitivity of the DEG UCPC to particle composition was also studied by comparing its response to positively charged 1.47 and 1.70 nm tetra-alkyl ammonium ions, sodium chloride, and silver particles. A high resolution differential mobility analyzer was used to generate the test particles. These results show that the response of this UCPC to sub-2 nm particles is sensitive to particle composition. The applicability of the new SMPS for atmospheric measurement was demonstrated during the Nucleation and Cloud Condensation Nuclei (NCCN) field campaign (Atlanta, Georgia, summer 2009). We operated the instrument at saturator and condenser temperatures that allowed the efficient detection of sodium chloride particles but not of air ions having the same mobility. We found that particles as small as 1 nm were detected during nucleation events but not at other times. Factors affecting size distribution measurements, including aerosol charging in the 1–10 nm size range, are discussed. For the charger used in this study, bipolar charging was found to be more effective for sub-2 nm particles than unipolar charging. No ion induced nucleation inside the charger was observed during the NCCN campaign.

Received 22 July 2010; accepted 12 September 2010.
This work was supported by a grant from US NSF (ATM-0506674) and US DOE grant DE-FG-05ER63997.
Address correspondence to Jingkun Jiang, School of Environmental Science & Engineering, Tsinghua University, Beijing, 100084 China. E-mail: jiangjk@tsinghua.edu.cn

INTRODUCTION

The scanning mobility particle spectrometer (SMPS) is the most commonly used instrument for measuring ultrafine aerosol size distributions (Wang and Flagan 1990). SMPS systems include an aerosol charger, a differential mobility analyzer (DMA), and an aerosol detector. Due to their high sensitivity and high signal-to-noise ratio, condensation particle counters (CPCs) have been widely used as detectors in SMPS systems (McMurry 2000). CPCs detect particles by exposing them to a supersaturated vapor (the "working fluid") that can condense on particles, causing them to grow to a size typically between 1 and 10 μm that can easily be detected by light scattering. The lower size limit of SMPS systems has been primarily limited by the minimum size that can be activated and detected with CPCs, which depends on the working fluid and CPC design. A butanol based laminar flow ultrafine condensation particle counter (UCPC) that was developed by Stolzenburg and McMurry (1991) and commercialized by TSI, Inc. (model 3025) detects particles as small as 2.5–3.0 nm. SMPS systems using this UCPC played an important role in the discovery that new particle formation occurs frequently throughout the atmosphere (Kulmala et al. 2004; McMurry et al. 2011).

Understanding mechanisms responsible for atmospheric nucleation has been driving the development of sub-2 nm aerosol instruments (McMurry et al. 2011). Nucleation can lead to the widespread formation of new particles and the enhanced concentrations of cloud condensation nuclei (CCN) in the atmosphere (Spracklen et al. 2008; Chang et al. 2009; Kuang et al. 2009). The International Panel on Climate Change has identified the cloud albedo effect as a major potential source of global cooling with larger uncertainties than any other climate forcing mechanism (IPCC 2007). CCN formed by nucleation likely influence the cloud albedo effect, and the effects of nucleation on CCN production and albedo need to be included in climate models. Size distribution measurements of particles smaller than 2 nm

will help to better understand the processes that lead to atmospheric nucleation and to reduce climate model uncertainties. In addition, the measurement of sub-2 nm particles has applications to fields beyond atmospheric research including nanoscale analytical chemistry (Fernández de la Mora et al. 1998; Fernández de la Mora 2011), nanomaterial synthesis (Jiang et al. 2007; Thimsen and Biswas 2007), and nanoparticle health effects (Oberdorster et al. 2005; Jiang et al. 2008).

Since 2000, the use of different condensing vapors and different instrument designs has extended the CPC minimum detectable size towards 1 nm. Activating sub-2 nm sodium chloride particles and molecular ions has been demonstrated in steady-flow mixing type CPCs using dibutyl phthalate and ethylene glycol (Gamero-Castano and Fernández de la Mora 2000, 2002; Kim et al. 2003; Sgro and Fernández de la Mora 2004). Winkler et al. (2008a, b) reported measurement of particles smaller than 2 nm using n-propanol in an expansion chamber. When operated at saturation ratios leading to self-nucleation, butanol CPCs can also activate sub-2 nm particles (Sipila et al. 2009). Magnusson et al. (2003) theoretically studied 30 different working fluids and recommended that working fluids having high surface tension (e.g., water and glycerol) could potentially lower the size limit of CPCs. By theoretically examining 863 working fluids in laminar flow UCPCs, Iida and coworkers (2009) concluded that working fluids with high surface tensions and low vapor pressures are best suited for detecting $\sim$1 nm particles. They then experimentally demonstrated that diethylene glycol (DEG; high surface tension) and oleic acid (low vapor pressure) can activate particles as small as 1 nm without undergoing self-nucleation. Following the study by Iida et al. (2009), Sipilä et al. (2010) have developed an improved mixing-type CPC (Sgro and Fernández de la Mora 2004) using diethylene glycol as the working fluid for sub-2 nm particle detection. Among different instrument designs, the laminar flow UCPC has proven its stability for long-term operation, which is critical for atmospheric field measurements.

In this article we describe the design and performance of a prototype SMPS utilizing the diethylene glycol UCPC for measurement of atmospheric particles down to mobility diameters close to 1 nm. We refer to this instrument system as the DEG SMPS. We chose DEG over oleic acid as the working fluid in the UCPC for several reasons. The DEG UCPC has higher activation efficiencies for sub-2 nm particles than a similar UCPC that uses oleic acid as the working fluid. Furthermore, DEG is rather inert while oleic acid reacts with gas phase radicals and ozone (Docherty and Ziemann 2006; Reynolds et al. 2006), which may cause it to degrade over time. Finally, DEG is inexpensive and is readily available in high purity grades.

The procedures that we use to obtain size distributions of atmospheric particles with the DEG SMPS are discussed in this paper. It includes a description of laboratory studies of the size- and material-dependent response of the DEG UCPC, as well as the approach used to calculate diffusional losses of these small particles. Measurements of the DMA transfer functions are described in a separate paper (Jiang et al. 2011a). Conversion of raw DEG SMPS data to size distributions also requires knowledge of size-dependent charged fractions. We used the Po-210 charger described by Chen and Pui (1999), which can be operated in either the bipolar or unipolar charging mode. For atmospheric measurements carried out in the 2009 Nucleation and Cloud Condensation Nuclei (NCCN) campaign at the Jefferson St. site in Atlanta, Georgia, we found that charged fractions of sub-3.6 nm particles were higher for bipolar charging. Therefore, reported size distributions are based on measurements carried out with in the bipolar charging mode and inverted using the Fuchs' stationary-state bipolar charging theory (Fuchs 1963; Hoppel and Frick 1986; Wiedensohler 1988). Particle size distributions (1–10 nm) during atmospheric nucleation events measured by this new instrument are presented and compared with results ($>$3 nm) obtained using conventional SMPS systems.

THE DEG SMPS

Instrument Description

Figure 1 illustrates the prototype scanning mobility particle spectrometer (the DEG SMPS) designed for measuring atmospheric particles down to sizes close to 1 nm. Atmospheric aerosol was sampled at 20 lpm including a transport flow of 13 lpm to reduce the inlet losses. The sampling flow of 7 lpm was extracted along the axis to reduce diffusion losses, which have a greater effect near the walls for laminar flow. Large particles were subsequently removed by an impactor with 10 μm cutoff size to prevent their accumulation inside the system. Sampled particles then entered an aerosol charger based on the design of Chen and Pui (1999). The sheath air used in the original design was eliminated to maximize concentrations of charged particles. Instead, we used a higher sampling flowrate (7 lpm) to reduce particle losses inside the charger. The diameter of the cylindrical charger housing was increased from 3.8 to 6.0 cm and the ion production region was redesigned to securely hold six 0.5 mCi Po-210 radioactive ionizers (NRD LLC, Model 1U400). The larger housing and higher radioactivity compensate for the higher flow rate that we used. This charger can be used as either a unipolar or bipolar charger by turning on and off the voltage applied to the ion production region. A similar charger is used to sample atmospheric nanoparticles for chemical analysis (Smith et al. 2004; McMurry et al. 2009).

After the charger, sampled particles were classified using a TSI 3085 nano differential mobility analyzer (nanoDMA, Chen et al. 1998). A bypass flow of 5 lpm was used to reduce particle losses at the nanoDMA inlet. The nanoDMA was operated in a closed-loop for sheath and excess flows (15 lpm). The aerosol inlet flowrate was equal to the aerosol outlet flowrate (2 lpm). Negatively charged particles were selected in the nanoDMA by applying positive voltage to the central electrode. Accordingly, when operated in the unipolar mode, we applied negative voltage to the charger so that negative ions were generated and particles were negatively charged. The use of negatively charged particles offers two benefits. Due to the higher mobilities of

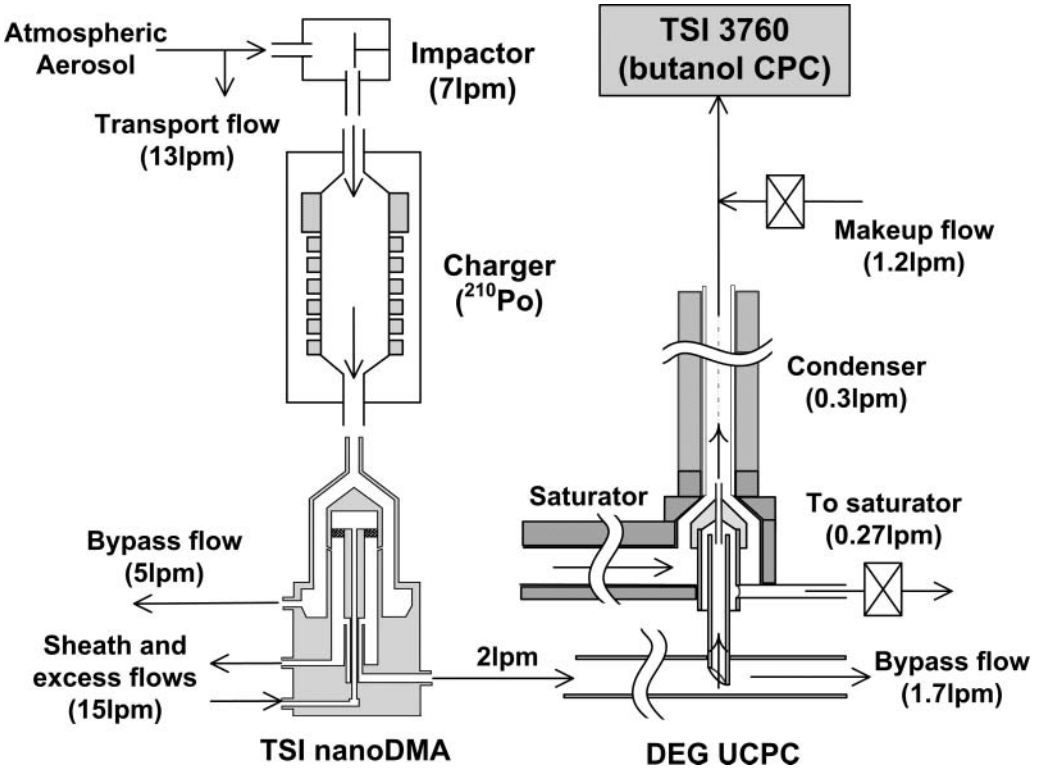

FIG. 1. Schematic of the scanning mobility particle spectrometer system using the DEG UCPC and a "booster" butanol CPC.

negative ions, negatively charged fractions exceed positively charged fractions for both unipolar and bipolar charging. Also, it has been observed that DEG activation efficiencies are higher for negative than positive sub-2 nm particles (Iida et al. 2009).

Classified particles were then sent into the detector consisting of the DEG UCPC and a TSI 3760 butanol CPC. The designs of the saturator/condenser for the DEG UCPC are the same as those used in the TSI 3025 UCPC and described by Stolzenburg and McMurry (1991), as is the flow control scheme with bypass, capillary, and condenser flowrates of 1.7, 0.03, and 0.3 lpm, respectively. The capillary flowrate was calibrated using the procedure given by Stolzenburg (1988). The saturator and condenser temperatures are monitored using thermocouples. The DEG UCPC was used to grow particles by heterogeneous condensation of DEG. The saturation vapor pressure of DEG within the UCPC condenser is about a factor of 100 lower than that of butanol. Consequently, the final droplet sizes after the DEG UCPC are correspondingly smaller than those achieved using a butanol UCPC and cannot be efficiently detected using light scattering. Therefore, the laser detection unit was removed, and a conventional butanol CPC, TSI 3760 with a 50% cutoff size at ~15 nm, was used as a "booster" after the DEG UCPC to further grow particles and to detect them individually using light scattering (Iida et al. 2009).

Data Inversion

Procedures for inverting DEG SMPS data to obtain number size distributions are similar to those used for other types of SMPS systems. Multiple charging effects are negligible for the particle size range measured by the DEG SMPS, i.e., 1–10 nm. The method proposed by Knutson (1976) and refined by Stolzenburg and McMurry (2008) was used for inverting the DEG SMPS data. Similar to Equation (27) in Stolzenburg and McMurry (2008), the unknown size distribution function is given by

$$\left.\frac{dN}{d\ ln D_p}\right|_{D_P^*} = \frac{N \cdot a^*}{\frac{Q_a}{Q_s} \cdot \beta \cdot (1+\delta) \cdot f_c(D_P^*) \cdot \eta_{ucpc}(D_P^*) \cdot \eta_{pene}(D_P^*)} \quad [1]$$

where N is the measured aerosol concentration downstream of the DEG UCPC; D_p is the particle diameter; $D_p{}^*$ is the diameter of a particle with the electrical mobility equal to nanoDMA transfer function centroid electrical mobility; Z_p is the particle electrical mobility; a^* has a value between 1 to 2, given by

$$a^* = (-d\ ln\ Z_p / d\ ln\ D_p)|_{D_P^*} \quad [2]$$

β and δ are given by

$$\beta = (Q_s + Q_a)/(Q_m + Q_c) \quad [3]$$

$$\delta = (Q_s - Q_a)/(Q_s + Q_a) \quad [4]$$

Q_a is the aerosol inlet flowrate; Q_s is the aerosol outlet flowrate; Q_c is the nanoDMA sheath flowrate; Q_m is the nanoDMA excess

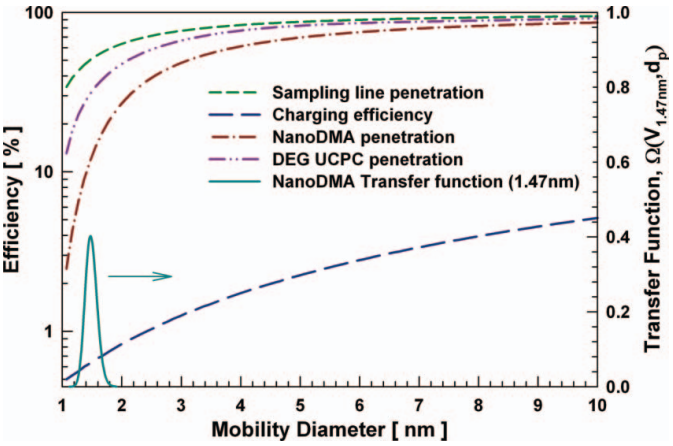

FIG. 2. Size-dependent particle transport efficiencies in the sampling lines, bipolar charging efficiencies (fractions of negatively charged particles carrying a single charge), nanoDMA penetration efficiencies, DEG UCPC penetration efficiencies, and the transfer function of the nanoDMA with a fixed DMA voltage for 1.47 nm particles.

flowrate; $f_c(D_p^*)$ is the fraction of charged particles; $\eta_{ucpc}(D_p^*)$ is the UCPC activation efficiency of particles with a diameter of D_p^*; $\eta_{pene}(D_p^*)$ is the product of particle penetration efficiencies through the sampling lines, the nanoDMA, and the DEG UCPC.

Figure 2 shows the size-dependent penetration efficiencies, bipolar charging efficiencies, and the nanoDMA transfer function with a fixed voltage for 1.47 nm particles. The transport efficiencies in the sampling lines were evaluated theoretically by assuming all the losses are due to laminar flow diffusion losses. It was assumed that bipolar charging rates given by Fuchs' stationary-state theory (Fuchs 1963; Hoppel and Frick 1986; Wiedensohler 1988) can be extrapolated down to 1 nm. TSI 3085 nanoDMA transfer functions and penetrations for sub-2 nm particles are discussed in a companion paper (Jiang et al. 2011a). Measured nanoDMA transfer functions agree very well with the diffusive transfer function theory (Stolzenburg 1988). The DMA inlet and outlet losses were also calculated using the laminar diffusional deposition model for cylindrical tubes. The effective lengths used for the inlet and outlet regions are 2.24 and 1.40 m, respectively. UCPC penetration efficiencies are determined by diffusional losses to the walls of the inner inlet tube and the capillary and were estimated using the model developed by Stolzenburg and McMurry (1991). DEG UCPC activation efficiencies were evaluated experimentally and are described in the next section. Figure 2 supports the assumption used by the above inversion method that the relative variation of the product $(dN/dlnD_p) \cdot f_c(D_p^*) \cdot \eta_{ucpc}(D_p^*) \cdot \eta_{pene}(D_p^*)$ is small across the non-zero width of the nanoDMA transfer function. Nearly identical results were obtained when a more complex linear inversion method was used (Hagen and Alofs 1983).

CHARACTERIZATION OF THE DEG UCPC

Method

Figure 3 shows the setup for calibrating the DEG UCPC performance. Two different methods were used to generate test nanoparticles. Monodisperse molecular mobility standards, tetra-heptyl ammonium monomer ions ($N^+[C_7H_{15}]_4$) and tetra-dodecyl ammonium monomer ions ($N^+[C_{12}H_{25}]_4$), were generated using an electrospray method and followed by mobility classification (Ude and Fernández de la Mora 2005). Their

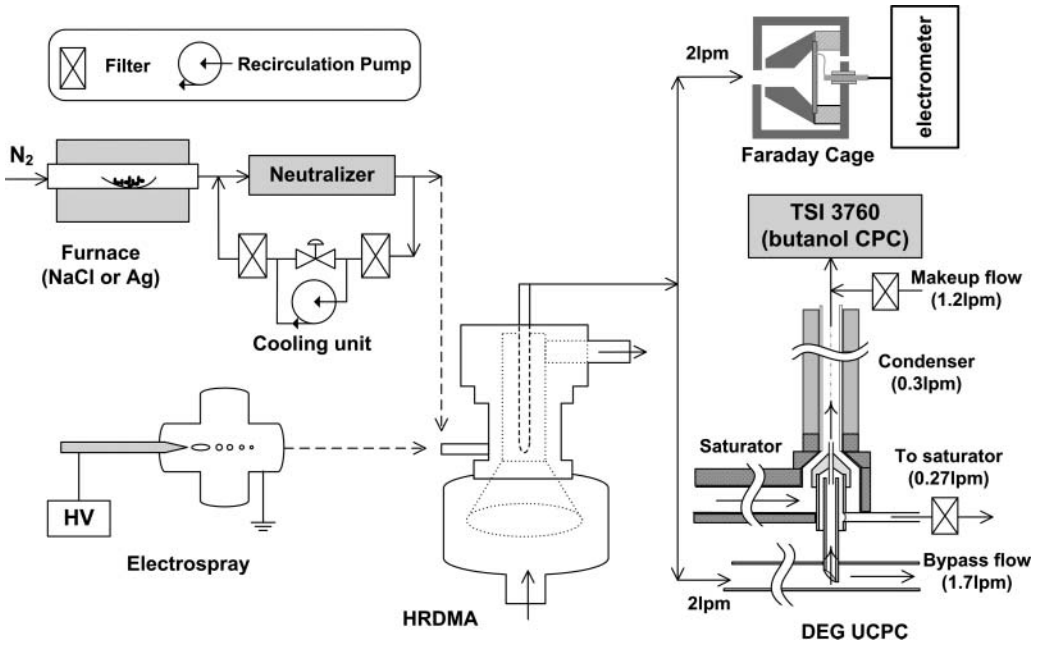

FIG. 3. Experimental setup for evaluating DEG UCPC activation efficiencies.

mobility diameters are 1.47 and 1.70 nm, respectively. The organic salts used to produce these ions (tetra-heptyl ammonium bromide (THABr, $N[C_7H_{15}]_4Br$) and tetra-dodecyl ammonium bromide (TDDABr, $N[C_{10}H_{21}]_4Br$)) were dissolved in ultrapure methanol with low concentrations (~few mM). Particle-free compressed air was used as the carrier gas. Sodium chloride (NaCl) and silver (Ag) nanoparticles were generated using the evaporation-condensation method (Scheibel and Porstendörfer 1983; Iida et al. 2009). A ceramic boat loaded with NaCl or Ag powders was placed in a high temperature ceramic tube furnace. By passing particle-free N_2 through the furnace tube, a NaCl or Ag vapor-rich stream was produced. Polydisperse NaCl or Ag nanoparticles were formed by quenching this hot vapor with the recirculating particle-free N_2 gas. Particles then flowed through a Po-210 neutralizer to bring them to a stationary charge distribution. The concentrations of the mobility-classified NaCl or Ag particles were significantly greater than the concentrations of ions downstream of the neutralizer, thereby ensuring that the reported activation efficiencies are representative of NaCl or Ag particles. All the chemicals, including the working fluid (DEG), were purchased and used as received from Sigma Aldrich.

A high resolution differential mobility analyzer (HRDMA) was used for particle classification to deliver monodisperse molecular ion standards and pseudo monodisperse NaCl and Ag nanoparticles. The HRDMA used in this study is also referred to as the Herrmann DMA (Herrmann et al. 2000) and it achieves resolutions as high as 70 for particles with mobility diameter of 1 nm (Fernández de la Mora 2011). The HRDMA was operated in an open-loop for sheath and excess flows and in a safe mode (the DMA outer electrode is grounded). The sheath flowrate was approximately 700 lpm. The HRDMA voltage-mobility relationship was calibrated using electrosprayed THABr ions prior to every experiment (Rosser and Fernández de la Mora 2005). Generated test particles were then transported to an aerosol electrometer (2 lpm) and the DEG UCPC (2 lpm). After the DEG UCPC, the TSI 3760 butanol CPC was used to further grow and count test particles. Both the DEG UCPC and the 3760 CPC were operated at the same flow schemes to those used in the DEG SMPS system.

A cylindrical wick formed from an 8×14 cm sheet of glass fiber filter was inserted into the DEG UCPC saturator. Due to its low vapor pressures, 10 ml DEG can last for more than two months under normal operating conditions. As previously reported by Iida et al. (2009), however, one source of instability of the DEG UCPC involves the condensation of water in the UCPC condenser and water absorption by DEG which can lead to large noise counts. Therefore, during both laboratory experiments and field campaigns we changed DEG no less than every 10 days and confirmed that the results were consistent before and after changing the working fluid. In addition, a 26 cm long Nafion semi-permeable membrane (PERMA PURE LLC) was installed in the DEG UCPC saturator flow (before the saturator) to reduce its relative humidity to values less than 20%.

UCPC counting efficiency at a given particle size is equal to the ratio of the particle concentration measured by the TSI 3760 to that measured by the aerosol electrometer (Liu and Pui 1974). Unlike previous studies that used DMAs with lower resolutions and explicitly accounted for polydispersity of test particles when evaluating size-dependent CPC counting efficiencies (Stolzenburg and McMurry 1991; Iida et al. 2009), measurements in this study were done on particles classified with the HRDMA and were therefore nearly monodisperse. Therefore, dispersion in size was not accounted for during data inversion. Since the droplet sizes after the DEG UCPC growth are larger than 100 nm (Iida et al. 2009) and droplets are far from the tube wall, it is reasonable to assume that their losses are negligible and that all particles activated in the DEG UCPC are detected by the TSI 3760. The UCPC counting efficiency can then be factored into the product of UCPC penetration efficiency and UCPC activation efficiency. The former is defined as the ratio of average particle concentration exiting the UCPC capillary to that entering the UCPC. The later is the fraction of particles exiting the UCPC capillary which are activated in the condenser. Again, UCPC penetration efficiencies are calculated using the model developed by Stolzenburg and McMurry (1991). UCPC activation efficiency can then be estimated from the measured UCPC counting efficiency.

Temperature Difference between UCPC Saturator and Condenser

DEG UCPC activation efficiencies for positively charged tetra-heptyl ammonium ions (1.47 nm mobility diameter) are shown in Figure 4. The DEG UCPC condenser temperature was 10°C. The activation efficiency for $N^+[C_7H_{15}]_4$ increased from ~0.5% to ~33.6% as the saturator-condenser temperature difference increased from 39.3 to 45.8°C. The temperature

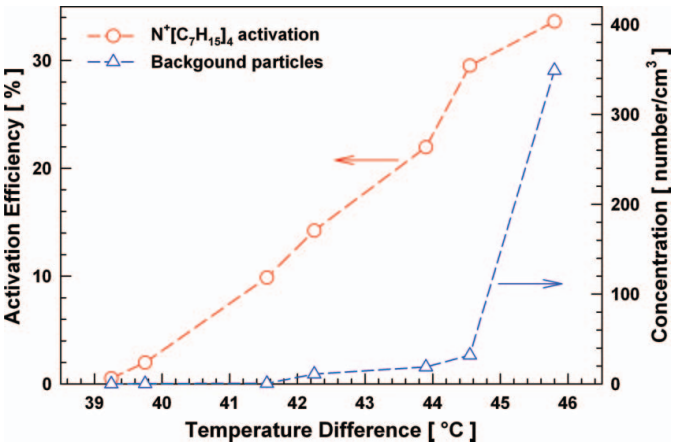

FIG. 4. DEG UCPC activation efficiencies of positively charged 1.47 nm tetra-heptyl ammonium ions and the number concentrations of the self-nucleated particles as a function of the saturator-condenser temperature difference. When estimating activation efficiencies, the contribution of self-nucleated particles is excluded. The condenser temperature was 10°C.

difference between the saturator and the condenser controls the vapor saturation ratio inside the condenser and therefore affects the activation efficiency. Larger temperature differences lead to higher saturation ratios and higher activation efficiencies. The self-nucleation rate of the working fluid also increases with increasing saturation ratio. When the self-nucleation rate is too high, "background particles" occur in the UCPC. As shown in Figure 4, the concentration of self-nucleated particles increases significantly when the temperature difference exceeds ~44.5°C. To avoid the potential interference between homogeneously nucleated particles and sampled particles, we prefer to operate UCPCs under conditions without self-nucleation of the working fluid, e.g., one background count per five minutes (~0.007 numbers/cm^3) is the criterion we used in previous studies (Stolzenburg and McMurry 1991; Iida et al. 2009). To stretch the capability of CPCs in detecting sub-2 nm particles, however, some studies have operated them with homogenous nucleation occurring inside the condenser (e.g., Mordas et al. 2008; Sipila et al. 2009). While some success was achieved in measuring well controlled laboratory aerosol systems, caution should be taken when measuring unknown aerosols (e.g., atmospheric aerosol). In this study, we used the same criterion, i.e., the background concentration is less than ~0.007 particles/cm^3, and operated the DEG UCPC at conditions without self-nucleation of the working fluid. The temperature difference of 39°C was used.

Activation Efficiencies of Different Materials

Figure 5 shows size-dependent activation efficiencies for positively charged sodium chloride, silver, and molecular ions at two discrete sizes (1.47 and 1.70 nm). For each material, particles of the same size were selected using the HRDMA, corresponding to the mobilities of the two molecular ion standards used ($N^+[C_7H_{15}]_4$ and $N^+[C_{12}H_{25}]_4$). The HRDMA was operated at a mobility resolution of about 25, corresponding to a size spread of about 8%. Particle concentrations were typically in the range of 10^3 cm^{-3}. The DEG UCPC was operated at the saturator-condenser temperature difference of 39°C. The data in Figure 5 show that the tendency of a working fluid to activate positively charged particles in the 1–2 nm size range depends strongly on both size and composition. Activation occurs most readily on NaCl followed by Ag. Only a small fraction of tetra-alkyl ammonium ions were activated. Activation efficiencies of positive ions generated inside the Po-210 neutralizer were also tested. For the three tested sizes (1.38, 1.47, and 1.58 nm), almost none of positive ions were activated by the DEG UCPC for these operating conditions.

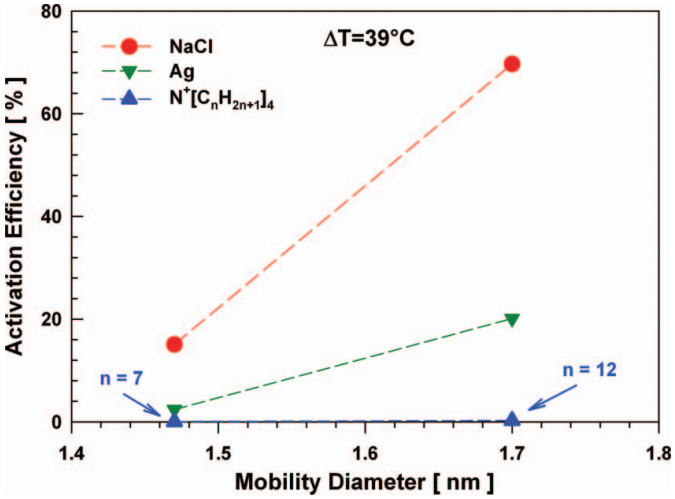

FIG. 5. DEG UCPC activation efficiencies of positively charged 1.47 and 1.70 nm particles carrying a single charge for three materials (sodium chloride, silver, and tetra-alkyl ammonium ions). The saturator and condenser temperatures were 49 and 10°C, respectively.

The condensational growth of particles smaller than ~3 nm can not be explained by particle size alone. Recent studies exposed WO_x nanoparticles in the 1 to 3 nm range to n-propanol and found that the saturation ratio required to initiate condensation decreases as the particle charge state changes from 0 to +1 to –1 (Winkler et al. 2008a). The preferential tendency of negatively charged particles to be activated was also observed by Wilson (1900) for water, by Kim et al. (2003) for ethylene glycol, and by Iida et al. (2009) for DEG and oleic acid. Winkler et al. (2008a) used Fletcher's heterogeneous condensation theory (Fletcher 1958) to explain the enhanced activation they observed for particles below 3 nm. However, Fletcher's theory can not explain the composition dependencies shown in Figure 5. Further studies are needed to better understand the effects of particle composition on heterogeneous condensation illustrated by the results in Figure 5.

The observed composition effects also depend on the condenser saturation ratio (i.e., the saturator-condenser temperature difference). Activation efficiencies for all materials would approach 100% if the saturation ratio were high enough. Under these conditions, activation efficiencies would be relatively insensitive to particle composition. Our laboratory measurements show that by operating the DEG UCPC under conditions that allow the activation of salt particles but not of air ions, we are able to distinguish charged salt particles from ions that are formed by ionizing radiation. Nano condensation nuclei (nano CN) are nanoparticles or molecular clusters that can be activated and detected with CPCs. As shown in Figures 4 and 5, whether or not an object with a given mobility is a nano CN depends not only on its composition but also on the CPC operating conditions. These dependencies might be exploited in the future to obtain information about the composition of mobility-classified atmospheric nano CN.

Activation Efficiencies for DEG SMPS Data Inversion

In calculating distribution functions of atmospheric particles measured by the DEG SMPS, it was assumed that their DEG UCPC activation efficiencies are equal to those for sodium chloride. Recent measurements show that nucleated clusters contain sulfuric acid (Zhao et al. 2010; Jiang et al. 2011b). They probably also contain a base, which could be ammonium or an amine

(Smith et al. 2010). The DEG UCPC activation efficiencies reported by Iida et al. (2009) for nanoparticles produced by nucleating vapors formed by vaporizing $(NH_4)_2SO_4$ are similar to NaCl activation efficiencies obtained in this study. Furthermore, based on chemical reasoning, Professor Ilja Siepmann (personal communication, Department of Chemistry, University of Minnesota, 2010) has suggested that the hydrogen bonding and other interactions that play a major role when working fluids such as DEG condense would be similar for such salts, but quite different from the interactions that would occur when DEG condenses on molecular ions or neutralizer ions or metals. While activation efficiencies of freshly nucleated particles are not known for certain, we believe it is reasonable, as a starting point, to assume that they behave similarly to sodium chloride. Clearly, the size-dependent activation efficiencies of freshly nucleated atmospheric particles ought to be measured directly.

Figure 6 shows size-dependent activation efficiencies for NaCl nanoparticles carrying a single negative charge measured in the laboratory using the apparatus shown in Figure 3. These results were obtained at the temperature difference of 39°C but with the saturator (T = 59°C) and the condenser temperatures (T = 20°C) each increased by 10°C relative to the values used for the experiments with positively charged particles (Figure 4). This was motivated by observations made during atmospheric field measurements. We found that when the condenser temperature was set at 10°C, the DEG UCPC and the TSI 3025 often malfunctioned when the relative humidity of the sampled air was high. Problems included clogging of the UCPC capillary and high background noise, which we attribute to the condensation of water inside the UCPC condenser and the absorption of water by the working fluids. A 26 cm long Nafion semi-permeable membrane was installed in the TSI 3025 UCPC saturator flow (before the saturator) to reduce its water content.

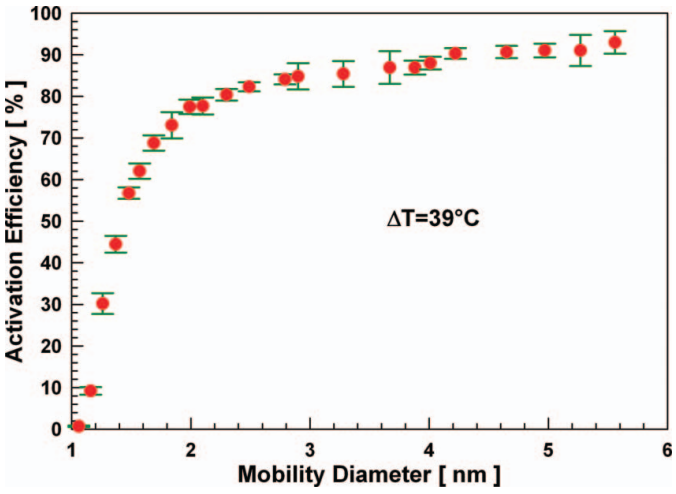

FIG. 6. DEG UCPC activation efficiencies of negatively charged 1 to 6 nm sodium chloride particles carrying a single charge. The saturator and condenser temperatures were 59 and 20°C, respectively.

For the DEG UCPC, the Nafion membrane did not solve the high background noise problem, so we increased its condenser temperature from 10 to 20°C. To keep the same saturator-condenser temperature difference (39°C), we also increased the saturator temperature from 49 to 59°C. As shown in Figure 6, NaCl particles as small as 1.1 nm mobility diameter are activated, albeit with low efficiency. The activation efficiency increases with size and becomes more than 90% at 6 nm. Because geometric sizes are about 0.3 nm smaller than mobility sizes (Ku and Fernández de la Mora 2009; Larriba et al. 2010), these results show that the DEG UCPC can activate sodium chloride particles with geometric sizes that are smaller than 1 nm. We also tested activation efficiencies of charger-generated negative ions at the same DEG UCPC operating conditions. At 1.16 nm, the activation efficiency of negative ions is ∼0.38% which is approximately 25 times less than NaCl particles with the same mobility diameter. The concentrations of ions from the Po-210 neutralizer at sizes larger than this were too low to be tested.

ATMOSPHRIC MEASUREMENTS

Method

During July and August 2009 we carried out the NCCN study at the Jefferson Street site in Atlanta, Georgia, where frequent and intense nucleation events are often observed (Woo et al. 2001; McMurry and Eisele 2005). The DEG SMPS was operated alongside a conventional particle size distribution (PSD) system consisting of a pair of aerosol mobility spectrometers operating in parallel (Woo et al. 2001). Both instrument systems were located in a sampling trailer. The DEG SMPS inlet penetrated through the north side of the trailer about 2 m above the ground. PSD samples were drawn through a sampling line that extended through the roof of the trailer to a height of about 4 m above the ground. The DEG SMPS measured the number distributions of particles in the 1–10 nm size range, while the PSD measured particles in the 3–500 nm size range. Both instruments were operated continuously and controlled through LABVIEW data acquisition programs. It took both instruments 5 min to complete an upscan and downscan measurement cycle. Their computer clocks were synchronized to Atlanta local standard time. The aerosol charger in the DEG SMPS was alternated between bipolar and unipolar modes after each measurement cycle (5 min). No voltage was applied to the DEG SMPS charger for measurements in the bipolar mode, while 2.4 kV negative voltage was applied for the unipolar mode measurements. The temperatures of DEG UCPC saturator and condenser were 59 and 20°C, respectively. DEG in the UCPC was changed at intervals of 10 days or less.

Bipolar Charging versus Unipolar Charging

Three sets of raw data from the DEG SMPS obtained on August 23 during nucleation events are shown in Figure 7. The aerosol charger in the DEG SMPS system was operated in the

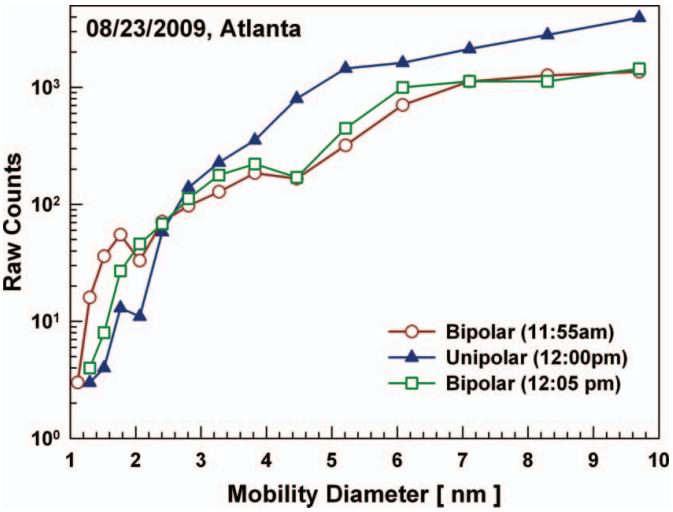

FIG. 7. Raw counts measured by the DEG SMPS while the aerosol charger was alternating between bipolar and unipolar modes.

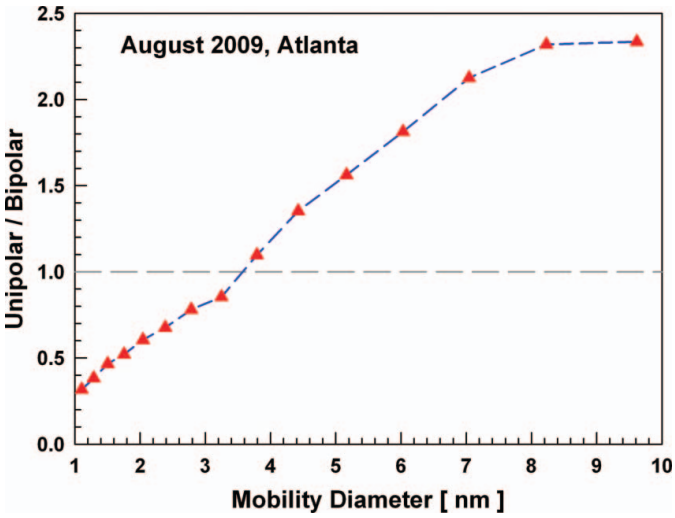

FIG. 8. Ratios of raw counts measured in the unipolar mode to those measured in the bipolar mode as a function of particle mobility diameter. We first added all the raw counts in a given size bin and in the same charging mode together and then calculated the ratio for this size bin. It includes data from six days in August 2009 when nucleation events occurred. Only data from event periods were used.

bipolar mode at 11:55 am and 12:05 pm and in the unipolar mode at 12:00 pm. For particles with mobility sizes larger than 2.4 nm, the counts detected in the unipolar mode are higher than those in the bipolar mode. For particles smaller than 2.4 nm, the unipolar mode reported lower raw counts than the bipolar mode. The data for particles larger than 2.4 nm are consistent with previous studies with this charger, which show that for particles larger than ~3 nm, the charged fractions produced in the unipolar mode exceed those for bipolar charging (Chen and Pui 1999; Smith et al. 2004; McMurry et al. 2009). However, there are no experiments to test its charging efficiencies for particles smaller than 3 nm.

To further verify this trend, we calculated the ratios of raw counts measured in the unipolar mode to those measured in the bipolar mode using the data from six days in August 2009 when nucleation events occurred. The results are shown in Figure 8. Only data from event periods were used and altogether more than twenty hours' data were used when calculating these ratios. The ratio increases from ~0.3 to ~2.3 as particle diameter increases from ~1 to ~10 nm. At approximately 3.6 nm, the charged fraction achieved in the unipolar mode is equal to that produced in the bipolar mode. This is slightly different from 2.4 nm shown in Figure 7, which includes measurements of only three size distributions. Variabilities in the unipolar/bipolar ratios occur due to variabilities in the measured size distributions during the measurement periods. Nevertheless, both figures illustrate that bipolar charging is more effective in measuring sub-2 nm atmospheric particles.

Chen and Pui (1999) operated the unipolar charger with a sheath flow to minimize electrostatic losses of charged nanoparticles. Because our objective was to maximize the concentration of charged particles downstream of the charger and not just to maximize the fraction of entering particles that acquired a charge, we operated the charger without a sheath flow. Without the sheath flow, electrostatic loss of charged particles in the unipolar mode might be higher than those originally estimated by Chen and Pui (1999). This loss is more severe for sub-2 nm particles due to their high mobilities. Therefore, it is possible that in this size range, though the unipolar mode might have higher intrinsic charging efficiencies (the probability of a particle to acquire charges regardless of whether this particle leaves the charger or gets lost inside the charger), its extrinsic charging efficiency (the probability of a particle to acquire charges and to leave the charger successfully) is lower than that of the bipolar mode when no voltage is applied to the charger. Another possibility is that due to the space charge effect, the average ion concentration to which nanoparticles are exposed is lower in the unipolar than in the bipolar modes. Bipolar charging results in lower charged fractions for large particles because of the bipolar charge environments. For sub-2 nm particles, bipolar charging produced higher charged fractions because so few particles acquire a charge that the reverse collision never has a chance. Larger particles, however, quickly acquire their first charge, allowing more time for the reverse collision to become important. Further studies on the charging efficiencies of sub-2 nm particles in this aerosol charger are needed to understand these size dependencies and to reduce the uncertainties caused by extrapolating bipolar charging rates down to 1 nm. In addition, as shown in Figure 2, the charging efficiency is the limiting factor of sub-2 nm particle measurement for the DEG SMPS within the detectable size range. An aerosol charger with higher charging efficiencies could improve the performance of the DEG SMPS significantly.

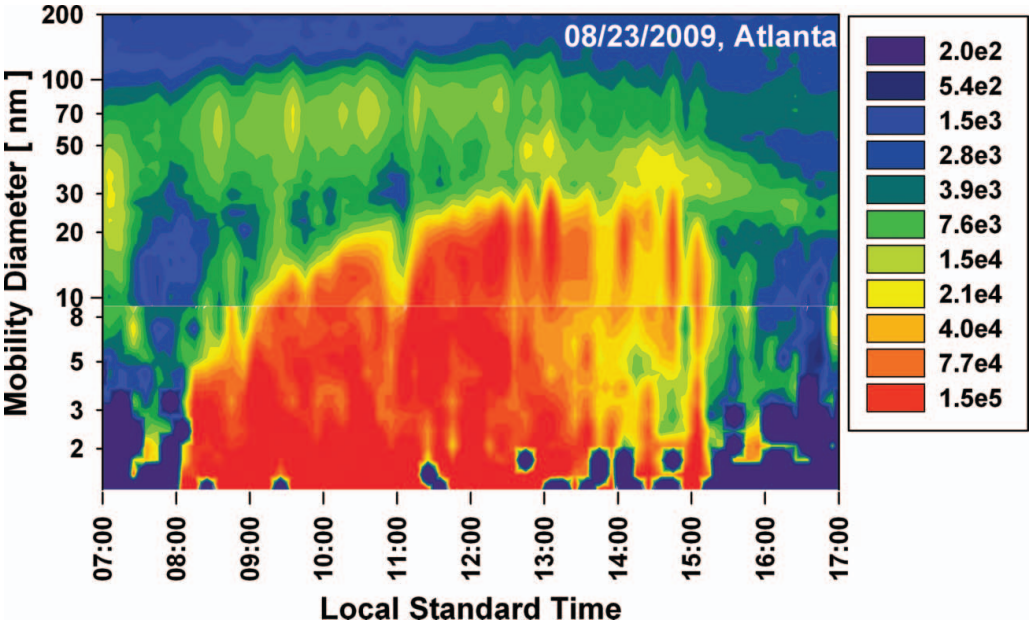

FIG. 9. A composite contour plot of particle number size distributions measured by the PSD (top, 9–200 nm) and by the DEG SMPS (bottom, 1–9 nm) during atmospheric nucleation events. The color indicates the values of the size distribution function ($dN/dlog_{10}D_p$, number/cm^3).

Particle Size Distributions during Nucleation Events

Figure 9 shows a composite contour plot of particle number distribution data ($dN/dlog_{10}D_p$, number/cm^3) from the DEG SMPS and the PSD obtained in Atlanta on August 23, 2009. On this day, nucleation was associated with solar radiation and sulfur dioxide (SO_2) emissions from the McDonough Steam Generating Plant, located 4.65 miles northwest from the sampling site. The estimated transport time from the source was ~50 min, and SO_2 concentrations of up to 30 ppbv were observed. This type of nucleation event is also referred to as a "plume" event (Kulmala et al. 2004; Sakurai et al. 2005). High concentrations of nanoparticles were formed photochemically as the plume was transported toward our sampling site, and freshly nucleated particles down to 1 nm were measured by the DEG SMPS. Due to the unknown charged fractions in the unipolar mode, only data from the bipolar mode are presented in Figure 9. PSD data from the same time period are used, so the presented size distributions were measured every 10 min instead of 5 min. As shown in Figure 9, very few sub-2 nm particles were detected before and after the nucleation event, while the concentrations of 1–2 nm particles increased dramatically during the event. The DEG SMPS and the PSD are in good agreement within the overlapping 3–10 nm size range (Jiang et al. 2011b). As discussed in a companion paper (Jiang et al. 2011b), good agreement was also observed between DEG SMPS data and nucleated clusters measured by a cluster chemical ionization mass spectrometer (Cluster CIMS, Zhao et al. 2010).

The estimated relative standard deviations of DEG SMPS reported size distributions are ~10% at 3 nm and ~50% at 1 nm (Jiang et al. 2011b). As mentioned above, size distributions that we report are based on the assumptions that charged fractions can be calculated using Fuchs' stationary-state theory and that activation efficiencies are equal to those for negatively charged NaCl.These assumptions lead to uncertainties that are difficult to quantify. As was shown in Figure 5, DEG UCPC activation efficiencies depend on particle composition. The smallest molecular clusters formed by nucleation overlap in mobility with small ions formed by radioactive decay and cosmic radiation. However, they are different in composition. Ions formed by the Po-210 source used in the charger are probably similar in composition to atmospheric ions, although subtle differences are likely (Eisele et al. 2006). As discussed earlier, laboratory experiments show that NaCl activation efficiencies are much higher than activation efficiencies of ions formed in the charger. We have not yet carried out field measurements that show how the DEG SMPS responds to ~1 nm ions formed by cosmic radiation or radioactive decay, and to ~1 nm freshly nucleated particles. However, while small ions of ~1 nm are always present in the atmosphere (Iida et al. 2006), the DEG SMPS detected ~1 nm objects only during new particle formation events (Jiang et al. 2011b). This observation leads us to conclude that the DEG SMPS detects nucleated particles of a given size with far higher efficiencies than small ions of the same size. This difference in detection efficiencies for ions and particles may be analogous to the material-dependent detection efficiencies shown in Figure 5. If the DEG UCPC efficiently detects freshly nucleated particles but not ions, as we surmise, this would be a fortuitous result that would largely eliminate the interference of small ions for DEG SMPS measurements of nanoparticle size distributions. Furthermore, composition is also likely to affect charged fractions for

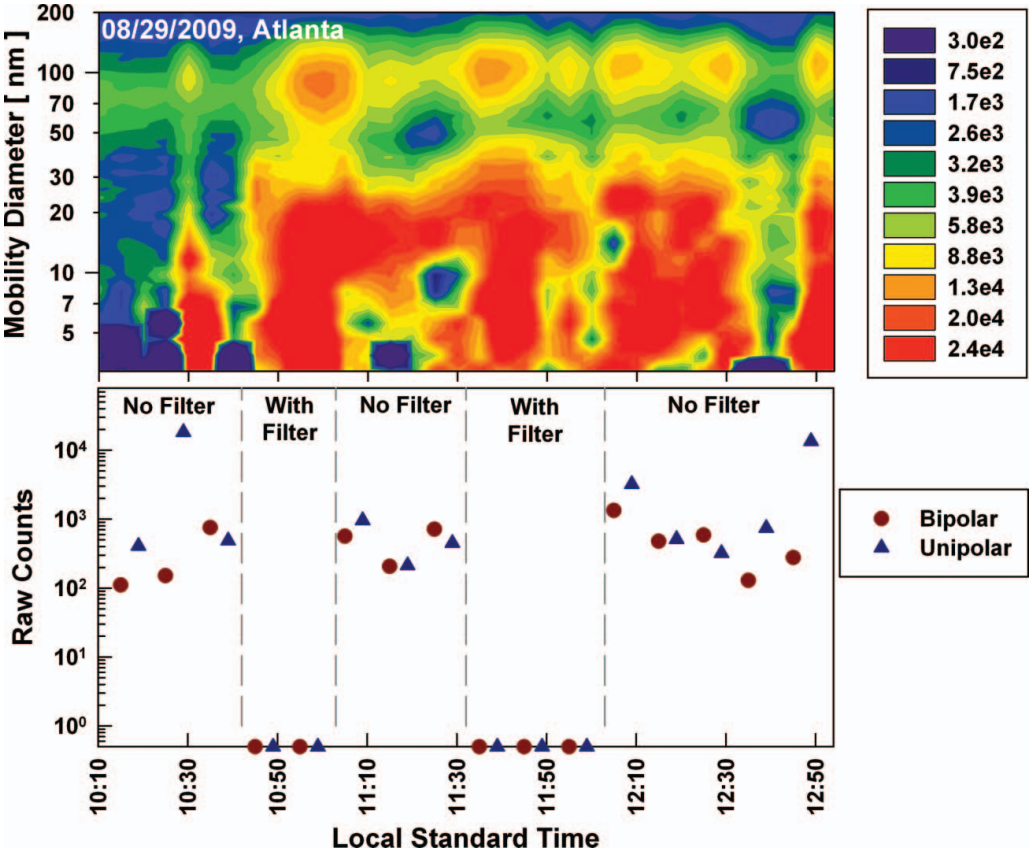

FIG. 10. A contour plot of particle number size distributions ($dN/dlog_{10}D_p$, number/cm^3) measured by the PSD (top, 3–200 nm) and total raw counts simultaneously measured by the DEG SMPS (bottom, 1–10 nm) with and without a filter at the sampling inlet while the aerosol charger was alternating between bipolar and unipolar modes. The values for those data points that are below one count are actually zero. In order to show them on the logarithm scale, their values were set to be 0.5.

very small particles. For example, the Cluster CIMS relies on the transfer of charge from the NO_3^- reagent ions to molecules or clusters that are more electronegative. If charge transfer to some nucleated clusters does not occur, then they would not be detected with the Cluster CIMS. Similarly, when particle composition affects charged fractions, Fuchs' stationary-state theory can no longer be used to determine charged fractions of nanoparticles. Clearly, more work is needed to study the effects of such material dependencies on the performance of instruments such as the DEG SMPS for particles in the ~1 nm range, and this will require a better understanding of nanoparticle composition.

Ion Induced Nucleation Inside the Charger

The possibility that ion induced nucleation inside the charger affects DEG SMPS measurements was also tested during the NCCN campaign. Iida et al. (2008) observed that ionizing radiation inside a conventional Po-210 neutralizer led to the formation of particles smaller than 4 nm during measurements in Mexico City. This artifact was strongly associated with the concentration of sulfur dioxide. To test whether this was occurring in our system, an acrylic copolymer HEPA filter (Pall Corporation, Model 12144) was installed at the DEG SMPS inlet to remove all particles in the sampled air. Figure 10 shows both the particle size distributions measured by the PSD and the total raw counts measured by the DEG SMPS on August 29, 2009. On this day, nucleation was caused by SO_2 emissions from upwind coal-fired power plants. When the filter was installed at the inlet of the DEG SMPS, its raw counts went to zero even when SO_2 concentrations were elevated and the PSD was detecting high concentrations of newly formed particles. When the filter was removed, the raw counts went back up again. This is valid for both bipolar and unipolar modes. We repeated this test several times and ion induced nucleation was never observed inside the DEG SMPS aerosol charger. Although we found no evidence for ion-induced nucleation during NCCN measurements, the earlier work of Iida et al. (2008) in Mexico City illustrates the need to determine for each sampling environment whether or not this process affects measurements. Furthermore, because the filter likely removes sulfuric acid vapor, this experiment does not definitively rule out the possibility that ion-induced nucleation of ambient sulfuric acid in the neutralizer could have affected our measurements. However, the filter likely did not remove sulfur dioxide, and most previous

studies of ion-induced nucleation in radioactive chargers suggest an association with sulfur dioxide (e.g., Hanson 2005).

This test also confirmed that at the selected saturation ratio (i.e., the saturator-condenser temperature of 39°C), the DEG UCPC measures freshly nucleated atmospheric particles with no interference from ions generated by the Po-210 source in the aerosol charger. When the filter was installed at the DEG SMPS inlet, no counts were observed which means that these ions are not activated by the DEG UCPC.

SUMMARY

The design and performance of a scanning mobility particle spectrometer equipped with a diethylene glycol ultrafine condensation particle counter for measuring size distributions of sub-2 nm atmospheric particles was described. Factors affecting size distribution measurement include DEG UCPC activation efficiencies, particle charging efficiencies, DMA transfer function, and transport efficiencies through sampling lines and different instruments. The DEG UCPC activation efficiencies of sub-2 nm particles of a given size are the highest for sodium chloride, followed by silver and tetra-alkyl ammonium ions. In the DEG SMPS charger, the extrinsic charging efficiencies of sub-2 nm particles are higher in the bipolar mode than in the unipolar mode. We demonstrated the feasibility of the DEG SMPS for long-term, continuous, and automated atmospheric field measurement. Number distribution functions of 1–10 nm particles were measured by the DEG SMPS during atmospheric nucleation events. Good agreement was observed between these data and results from conventional SMPS systems (3–500 nm). Utilizing these DEG SMPS data to obtain fundamental new information about nucleation and growth rates of atmospheric particles is a focus of our ongoing research.

REFERENCES

Chang, L. S., Schwartz, S. E., McGraw, R., and Lewis, E. R. (2009). Sensitivity of Aerosol Properties to New Particle Formation Mechanism and to Primary Emissions in a Continental-Scale Chemical Transport Model. *J. Geophys. Res. Atmospheres.* 114:D07203.

Chen, D.-R., and Pui, D. Y. H. (1999). A High Efficiency, High Throughput Unipolar Aerosol Charger for Nanoparticles. *J. Nanoparticle Res.* 1:115–126.

Chen, D. R., Pui, D. Y. H., Hummes, D., Fissan, H., Quant, F. R., and Sem, G. J. (1998). Design and Evaluation of a Nanometer Aerosol Differential Mobility Analyzer (Nano-DMA). *J. Aerosol Sci.* 29:497–509.

Docherty, K. S., and Ziemann, P. J. (2006). Reaction of Oleic Acid Particles with NO3 Radicals: Products, Mechanism, and Implications for Radical-Initiated Organic Aerosol Oxidation. *J. Phys. Chem. A.* 110:3567–3577.

Eisele, F. L., Lovejoy, E. R., Kosciuch, E., Moore, K. F., Mauldin, R. L., Smith, J. N., McMurry, P. H., and Iida, K. (2006). Negative Atmospheric Ions and Their Potential Role in Ion-Induced Nucleation. *J. Geophys. Res. Atmospheres.* 111:D04305.

Fernández de la Mora, J. (2011). Sub-3 nm Aerosol Measurement with DMAs and CNCs, in *Aerosol Measurement: Principles, Techniques, and Applications*, P. Kulkarni, P. A. Baron, and K. Willeke, eds., John Wiley & Sons, New York, pp. 697–722.

Fernández de la Mora, J., de Juan, L., Eichler, T., and Rosell, J. (1998). Differential Mobility Analysis of Molecular Ions and Nanometer Particles. *Trac-Trends in Anal. Chem.* 17:328–339.

Fletcher, N. H. (1958). Size Effect in Heterogeneous Nucleation. *J. Chem. Phys.* 29:572–576.

Fuchs, N. A. (1963). On the Stationary Charge Distribution on Aerosol Particles in a Bipolar Ionic Atmosphere. *Geofis. Pura. Appl.* 56:185–193.

Gamero-Castano, M., and Fernández de la Mora, J. (2000). A Condensation Nucleus Counter (CNC) Sensitive to Singly Charged Sub-Nanometer Particles. *J. Aerosol Sci.* 31:757–772.

Gamero-Castano, M., and Fernández de la Mora, J. (2002). Ion-Induced Nucleation: Measurement of the Effect of Embryo's Size and Charge State on the Critical Supersaturation. *J. Chem. Phys.* 117:3345–3353.

Hagen, D. E., and Alofs, D. J. (1983). Linear Inversion Method to Obtain Aerosol Size Distributions from Measurements with a Differential Mobility Analyzer. *Aerosol Sci. Technol.* 2:465–475.

Hanson, D. R. (2005). Mass Accommodation of H2SO4 and CH3SO3H on Water-Sulfuric Acid Solutions from 6% to 97% RH. *J. Phys. Chem. A.* 109:6919–6927.

Herrmann, W., Eichler, T., Bernardo, N., and Fernández de la Mora, J. (2000). Turbulent Transition Arises at Reynolds Number 35,000 in a Short Vienna Type DMA with a Large Laminarization Inlet. *AAAR Annual Conference*, St. Louis, Missouri, USA.

Hoppel, W. A., and Frick, G. M. (1986). Ion-Aerosol Attachment Coefficients and the Steady-State Charge Distribution on Aerosols in a Bipolar Ion Environment. *Aerosol Sci. Technol.* 5:1–21.

Iida, K., Stolzenburg, M., McMurry, P., Dunn, M. J., Smith, J. N., Eisele, F., and Keady, P. (2006). Contribution of Ion-Induced Nucleation to New Particle Formation: Methodology and Its Application to Atmospheric Observations in Boulder, Colorado. *J. Geophys. Res. Atmospheres.* 111:D23201.

Iida, K., Stolzenburg, M. R., and McMurry, P. H. (2009). Effect of Working Fluid on Sub-2 nm Particle Detection with a Laminar Flow Ultrafine Condensation Particle Counter. *Aerosol Sci. Technol.* 43:81–96.

Iida, K., Stolzenburg, M. R., McMurry, P. H., and Smith, J. N. (2008). Estimating Nanoparticle Growth Rates from Size-Dependent Charged Fractions: Analysis of New Particle Formation Events in Mexico City. *J. Geophys. Res. Atmospheres.* 113:D05207.

IPCC. (2007). Climate Change 2007: IPCC Fourth Assessment Report (AR4), Cambridge University Press.

Jiang, J., Attoui, M., Heim, M., Brunell, N. A., McMurry, P. H., Kasper, G., Flagan, R. C., Giapis, K., and Mouret, G. (2011a). Transfer Functions and Penetrations of Five Differential Mobility Analyzers for Sub-2 nm Particle Classification. *Aerosol Sci. Technol.* 45:480–492.

Jiang, J., Chen, D. R., and Biswas, P. (2007). Synthesis of Nanoparticles in a Flame Aerosol Reactor with Independent and Strict Control of Their Size, Crystal Phase, and Morphology. *Nanotechnology.* 18:285603.

Jiang, J., Oberdörster, G., Elder, A., Gelein, R., Mercer, P., and Biswas, P. (2008). Does Nanoparticle Activity Depend upon Size and Crystal Phase? *Nanotoxicology.* 2:33–42.

Jiang, J., Zhao, J., Chen, M., Scheckman, J., Williams, B. J., Kuang, C., Eisele, F., and McMurry, P. (2011b). First Measurements of Neutral Atmospheric Cluster and 1–2 nm Particle Number Size Distributions during Nucleation Events. *Aerosol Sci. Technol.* (in press).

Kim, C. S., Okuyama, K., and Fernández de la Mora, J. (2003). Performance Evaluation of an Improved Particle Size Magnifier (PSM) for Single Nanoparticle Detection. *Aerosol Sci. Technol.* 37:791–803.

Knutson, E. O. (1976). Extended Electric Mobility Method for Measuring Aerosol Particle Size and Concentration, in *Fine Particles: Aerosol Generation, Measurement, Sampling, and Analysis*, B. Y. H. Liu, ed., Academic Press, New York, pp. 739–762.

Ku, B. K., and Fernández de la Mora, J. (2009). Relation between Electrical Mobility, Mass, and Size for Nanodrops 1–6.5 nm in Diameter in Air. *Aerosol Sci. Technol.* 43:241–249.

Kuang, C., McMurry, P. H., and McCormick, A. V. (2009). Determination of Cloud Condensation Nuclei Production from Measured New Particle Formation Events. *Geophys. Res. Lett.* 36:L09822.

Kulmala, M., Vehkamaki, H., Petaja, T., Dal Maso, M., Lauri, A., Kerminen, V. M., Birmili, W., and McMurry, P. H. (2004). Formation and Growth Rates

of Ultrafine Atmospheric Particles: A Review of Observations. *J. Aerosol Sci.* 35:143–176.

Larriba, C., Hogan, Jr., C. J., Attoui, M., Borrajo, R., Garcia, J. F., and Fernández de la Mora, J. (2011). The Mobility-Volume Relationship below 3.0 nm Examined by Tandem Mobility-Mass Measurement. *Aerosol Sci. Technol.* 45:453–467.

Liu, B. Y. H., and Pui, D. Y. H. (1974). A Submicron Aerosol Standard and the Primary, Absolute Calibration of the Condensation Nuclei Counter. *J. Colloid Interface Sci.* 47:155–171.

Magnusson, L. E., Koropchak, J. A., Anisimov, M. P., Poznjakovskiy, V. M., and Fernández de la Mora, J. (2003). Correlations for Vapor Nucleating Critical Embryo Parameters. *J. Phys. Chem. Ref. Data.* 32:1387–1410.

McMurry, P. H. (2000). The History of Condensation Nucleus Counters. *Aerosol Sci. Technol.* 33:297–322.

McMurry, P. H., and Eisele, F. L. (2005). Preface to Topical Collection on New Particle Formation in Atlanta. *J. Geophys. Res. Atmospheres.* 110:D22s01.

McMurry, P. H., Ghimire, A., Ahn, H. K., Sakurai, H., Moore, K., Stolzenburg, M., and Smith, J. N. (2009). Sampling Nanoparticles for Chemical Analysis by Low Resolution Electrical Mobility Classification. *Environ. Sci. Technol.* 43:4653–4658.

McMurry, P. H., Kuang, C., Smith, J. N., Zhao, J., and Eisele, F. (2011). Atmospheric New Particle Formation: Physical and Chemical Measurements, in *Aerosol Measurement: Principles, Techniques, and Applications*, P. Kulkarni, P. A. Baron, and K. Willeke, eds., John Wiley & Sons, New York, pp. 681–696.

Mordas, G., Sipila, M., and Kulmala, M. (2008). Nanometer Particle Detection by the Condensation Particle Counter UF-02proto. *Aerosol Sci. Technol.* 42:521–527.

Oberdorster, G., Oberdorster, E., and Oberdorster, J. (2005). Nanotoxicology: An Emerging Discipline Evolving from Studies of Ultrafine Particles. *Environ. Health Perspect.* 113:823–839.

Reynolds, J. C., Last, D. J., McGillen, M., Nijs, A., Horn, A. B., Percival, C., Carpenter, L. J., and Lewis, A. C. (2006). Structural Analysis of Oligomeric Molecules Formed from the Reaction Products of Oleic Acid Ozonolysis. *Environ. Sci. Technol.* 40:6674–6681.

Rosser, S., and Fernández de la Mora, J. (2005). Vienna-Type DMA of High Resolution and High Flow Rate. *Aerosol Sci. Technol.* 39:1191–1200.

Sakurai, H., Fink, M. A., McMurry, P. H., Mauldin, L., Moore, K. F., Smith, J. N., and Eisele, F. L. (2005). Hygroscopicity and Volatility of 4–10 nm Particles during Summertime Atmospheric Nucleation Events in Urban Atlanta. *J. Geophys. Res. Atmospheres.* 110:D22s04.

Scheibel, H. G., and Porstendörfer, J. (1983). Generation of Monodisperse Ag- and NaCl-Aerosols with Particle Diameters between 2 and 300 nm. *J. Aerosol Sci.* 14:113–126.

Sgro, L. A., and Fernández de la Mora, J. (2004). A Simple Turbulent Mixing CNC for Charged Particle Detection Down to 1.2 nm. *Aerosol Sci. Technol.* 38:1–11.

Sipilä, M., Berndt, T., Petaja, T., Brus, D., Vanhanen, J., Stratmann, F., Patokoski, J., Mauldin, R. L., Hyvarinen, A. P., Lihavainen, H., and Kulmala, M. (2010). The Role of Sulfuric Acid in Atmospheric Nucleation. *Science.* 327:1243–1246.

Sipila, M., Lehtipalo, K., Attoui, M., Neitola, K., Petmaja, T., Aalto, P. P., O'Dowd, C. D., and Kulmala, M. (2009). Laboratory Verification of PH-CPC's Ability to Monitor Atmospheric Sub-3 nm Clusters. *Aerosol Sci. Technol.* 43:126–135.

Smith, J. N., Barsanti, K. C., Friedli, H. R., Ehn, M., Kulmala, M., Collins, D. R., Scheckman, J. H., Williams, B. J., and McMurry, P. H. (2010). Observations of Aminium Salts in Atmospheric Nanoparticles and Possible Climatic Implications. *Proc. Natl. Acad. Sci. USA.* 107:6634–6639.

Smith, J. N., Moore, K. F., McMurry, P. H., and Eisele, F. L. (2004). Atmospheric Measurements of Sub-20 nm Diameter Particle Chemical Composition by Thermal Desorption Chemical Ionization Mass Spectrometry. *Aerosol Sci. Technol.* 38:100–110.

Spracklen, D. V., Carslaw, K. S., Kulmala, M., Kerminen, V. M., Sihto, S. L., Riipinen, I., Merikanto, J., Mann, G. W., Chipperfield, M. P., Wiedensohler, A., Birmili, W., and Lihavainen, H. (2008). Contribution of Particle Formation to Global Cloud Condensation Nuclei Concentrations. *Geophys. Res. Lett.* 35:L06808.

Stolzenburg, M. (1988). An Ultrafine Aerosol Size Distribution Measuring System. University of Minnesota Twin Cities, Minneapolis.

Stolzenburg, M. R., and McMurry, P. H. (1991). An Ultrafine Aerosol Condensation Nucleus Counter. *Aerosol Sci. Technol.* 14:48–65.

Stolzenburg, M. R., and McMurry, P. H. (2008). Equations Governing Single and Tandem DMA Configurations and a New Lognormal Approximation to the Transfer Function. *Aerosol Sci. Technol.* 42:421–432.

Thimsen, E., and Biswas, P. (2007). Nanostructured Photoactive Films Synthesized by a Flame Aerosol Reactor. *Aiche J.* 53:1727–1735.

Ude, S., and Fernández de la Mora, J. (2005). Molecular Monodisperse Mobility and Mass Standards from Electrosprays of Tetra-alkyl Ammonium Halides. *J. Aerosol Sci.* 36:1224–1237.

Wang, S. C., and Flagan, R. C. (1990). Scanning Electrical Mobility Spectrometer. *Aerosol Sci. Technol.* 13:230–240.

Wiedensohler, A. (1988). An Approximation of the Bipolar Charge-Distribution for Particles in the Sub-Micron Size Range. *J. Aerosol Sci.* 19:387–389.

Wilson, C. T. R. (1900). On the Comparative Efficiency as Condensation Nuclei of Positively and Negatively Charged Ions. *Philos. Trans. R. Soc. Lond. A.* 193:289–308.

Winkler, P. M., Steiner, G., Vrtala, A., Vehkamaki, H., Noppel, M., Lehtinen, K. E. J., Reischl, G. P., Wagner, P. E., and Kulmala, M. (2008a). Heterogeneous Nucleation Experiments Bridging the Scale from Molecular Ion Clusters to Nanoparticles. *Science.* 319:1374–1377.

Winkler, P. M., Vrtala, A., and Wagner, P. E. (2008b). Condensation Particle Counting Below 2 nm Seed Particle Diameter and the Transition from Heterogeneous to Homogeneous Nucleation. *Atmos. Res.* 90:125–131.

Woo, K. S., Chen, D. R., Pui, D. Y. H., and McMurry, P. H. (2001). Measurement of Atlanta Aerosol Size Distributions: Observations of Ultrafine Particle Events. *Aerosol Sci. Technol.* 34:75–87.

Zhao, J., Eisele, F. L., Titcombe, M., Kuang, C., and McMurry, P. H. (2010). Chemical Ionization Mass Spectrometric Measurements of Atmospheric Neutral Clusters Using the Cluster-CIMS. *J. Geophys. Res. Atmospheres.* 115:D08205.